Inorganic Chemistry

pubs.acs.org/IC
Communication

In Crystallo Hydrogenation of Nitrous Oxide Using a Rhodium(II) Hydride Complex

Thomas M. Hood, Sophie H. Dewick, Jie Liu, Emma Richards,* and Adrian B. Chaplin*

Cite This: https://doi.org/10.1021/acs.inorgchem.6c04272
Read Online

ABSTRACT: The stoichiometric and catalytic hydrogenation of nitrous oxide mediated by gas/solid reactions of rhodium(II) pincer complexes $[Rh(PNP\text{-}tBu)X]^+$ (X = CH_3, H, OH; PNP-*t*Bu = 2,6-$(tBu_2PCH_2)_2C_5H_3N$) is reported. A reaction sequence involving Rh(II)−CH_3 → Rh(II)−H → Rh(II)−OH → Rh(II)−H bond interconversions has been structurally mapped out by single-crystal X-ray diffraction and verified by EPR spectroscopy. These rhodium(II) metalloradicals are sufficiently robust to catalyze the hydrogenation of nitrous oxide at room temperature with modest productivity (8.3 apparent turnovers). The relative rates of the stoichiometric transformations suggest that Rh−O bond hydrogenolysis is turnover-limiting.

Nitrous oxide (N_2O) is a potent greenhouse gas and ozone depleting substance.[1] Within the nitrogen cycle, N_2O is consumed by denitrifying microorganisms through $2e^-/2H^+$ reduction to N_2 and H_2O, catalyzed by the copper-containing enzyme nitrous oxide reductase.[2] Hydrogenation is an alternative way of achieving this outcome in a lab setting but typically requires elevated temperatures and precious metal-based heterogeneous catalysts.[3] While O atom insertion into M−H bonds is an established N_2O activation manifold,[4] few transition metal complexes are known to catalyze the homogeneous hydrogenation of N_2O.[5−8] Hydrogenolysis by addition of H_2 across M−O bonds is not well-documented, and onward reactivity of metal hydroxides, such as those resulting from activation of N_2O, is generally induced by protonolysis (Figure 1A).[5,6,9]

Inspired by the work of Campos et al. on the organometallic chemistry of iridium(II) pincer complexes[10,11] and building upon developments in our laboratories,[7,12,13] we set about examining the hydrogenation of N_2O using the novel rhodium(II) hydride complex $[Rh(PNP\text{-}tBu)H][BAr^F{}_4]$ **1** (PNP-*t*Bu = 2,6-$(tBu_2PCH_2)_2C_5H_3N$, Ar^F = 3,5-$(CF_3)_2C_6H_3$), hypothesizing that reaction of H_2 with the open-shell hydroxide derivative $[Rh(PNP\text{-}tBu)(OH)][BAr^F{}_4]$ **2** would be promoted by metalloradical reactivity (Figure 1B). The closest literature precedent for **1** is a square-pyramidal rhodium(II) hydride prepared in solution by one-electron oxidation of $[Rh(PPh_3)_3(CO)H]$.[14] Attempts to access **1** in a similar manner, however, invariably afforded diamagnetic $[Rh(PNP\text{-}tBu)(H_2)][BAr^F{}_4]$ **3** as the common organometallic product. Recognizing the propensity of the open-shell hydride for intermolecular decomposition in solution, we turned to solid-state molecular organometallic methods to study **1** and assess our hypothesis through gas/solid reactions.[15,16] We herein report on the *in crystallo* hydrogenation of N_2O and characterization of the metalloradical intermediates involved in this transformation by single-crystal X-ray diffraction and EPR spectroscopy.

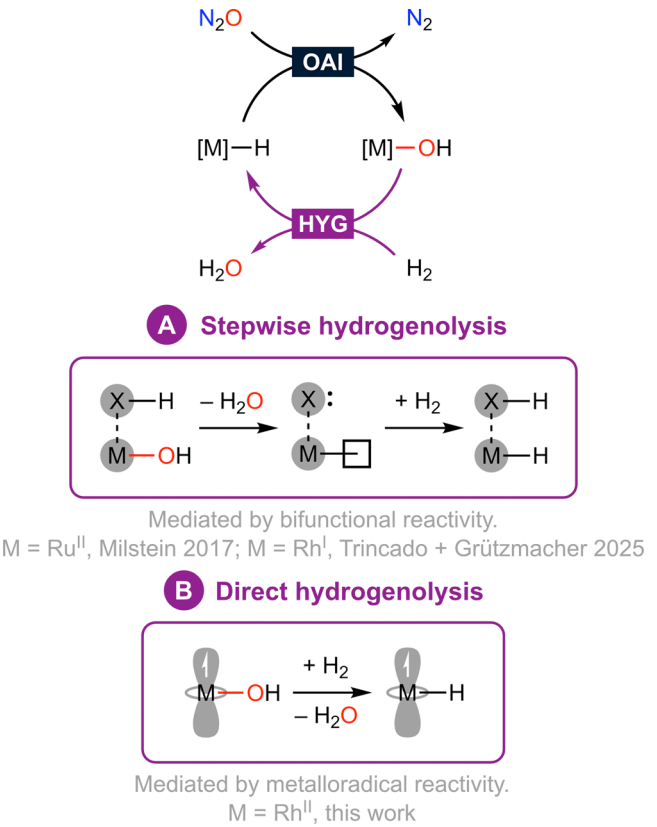

Figure 1. Transition metal catalyzed hydrogenation of N_2O proceeding by O atom insertion (OAI) into a M−H bond followed by (A) stepwise or (B) direct hydrogenolysis (HYG) of the resulting M−OH bond.

Received: August 11, 2026
Revised: August 18, 2026
Accepted: August 21, 2026

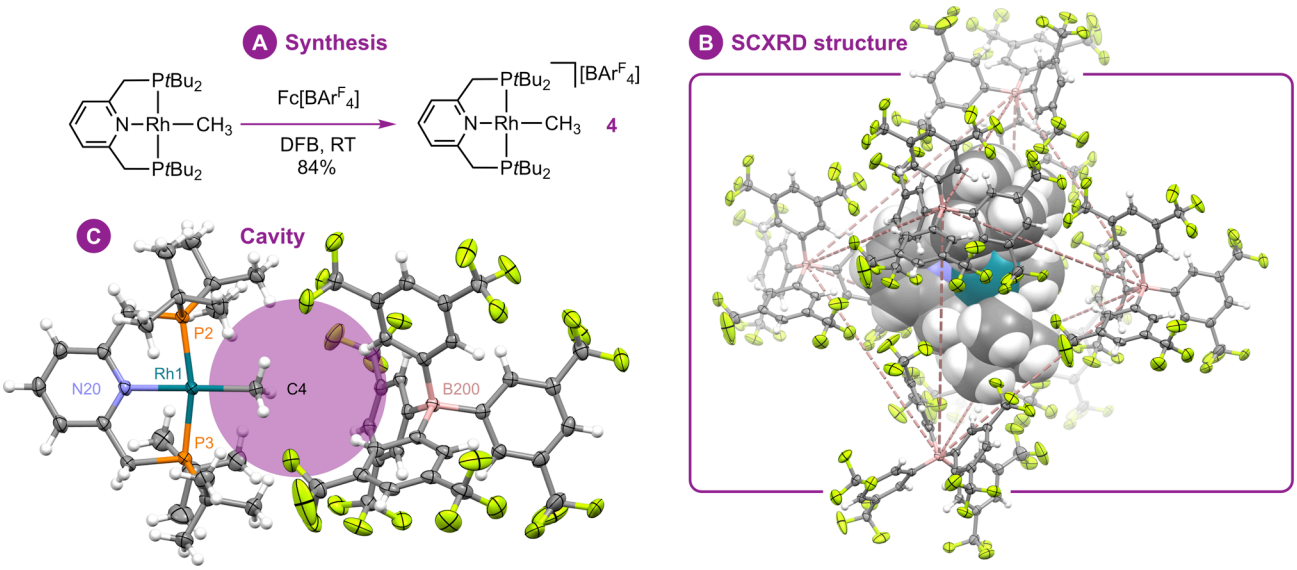

Figure 2. (A) Synthesis and (B, C) structural characterization of rhodium(II) methyl complex **4**. Insert (B) illustrates packing of the cation (rendered in space fill) within an octahedral arrangement of anions. Insert (C) illustrates positioning of the methyl ligand within the cleft of the proximal $[BAr^F_4]^-$ counterion. Thermal ellipsoids at 50% probability and minor disordered components omitted for clarity (3 × CF_3 groups). Selected metrics: Rh1–P2, 2.3160(5) Å; Rh1–P3, 2.3148(5) Å; Rh1–N20, 2.151(2) Å; Rh1–C4, 2.085(2) Å; Rh1–B200, 8.072(2) Å; P2–Rh1–P3, 165.61(2)°; N20–Rh1–C4, 177.73(9)°.

To synthesize **1** in the solid state, a strategy involving treatment of crystalline samples of novel rhodium(II) methyl complex $[Rh(PNP\text{-}t\text{Bu})(CH_3)][BAr^F_4]$ **4** with H_2 was devised. The required rhodium(II) precursor was subsequently obtained as dark purple microcrystalline powder following one-electron oxidation of the known rhodium(I) congener ($E_{1/2}$ = −0.64 V vs Fc^+/Fc, Fc = ferrocene) with $Fc[BAr^F_4]$ in 1,2-difluorobenzene (DFB, Figure 2A).[12,17] Complex **4** is stable in 2-methyltetrahydrofuran (MeTHF) solution at room temperature, and only ca. 10% decomposition was observed in DFB over 24 h, enabling single crystals of **4** suitable for analysis by X-ray diffraction to be reproducibly obtained by recrystallization from DFB/hexane at room temperature (monoclinic, $P2_1/c$). The resulting solid-state structure is notable for adoption of a square planar metal geometry and a Rh1–C4 distance of 2.094(3) Å. Each $[Rh(PNP\text{-}t\text{Bu})(CH_3)]^+$ cation is surrounded by an octahedral arrangement of $[BAr^F_4]^-$ anions, and the methyl ligand is notably projected into a cleft of the proximal counterion, which demarcates a cavity about this coordination site that is well-suited to gas/solid reactivity (Figure 2B,C).[15] Subsequent analysis of the bulk microcrystalline sample by powder X-ray diffraction confirmed exclusive adoption of this morphology. In DFB/MeTHF solution, the presence of a single paramagnetic species of C_{2v} symmetry is evident by ^{1}H NMR spectroscopy. All the proton environments can be located between δ −70 and +40, and an effective magnetic moment of 1.64 μ_B was determined in MeTHF using Evans' method,[18] consistent with the expected d^7-metal configuration. No ^{31}P resonance could be located between δ −600 and +600. Assignment as a metal-centered radical was subsequently corroborated by analysis of a frozen MeTHF glass solution of **4** by EPR spectroscopy at 115 K, with **4** observed alongside the corresponding square pyramidal solvent adduct **4**·MeTHF in a 1:1 ratio (Figure 3A). Complex **4** displays rhombic symmetry and a high degree of *g*-anisotropy (g_1 = 3.801, g_2 = 1.851, g_3 = 1.521; A_1 = 298 MHz, A_2 = 191 MHz, A_3 = 181 MHz from coupling to ^{103}Rh), characteristic of authentically square planar rhodium(II) complexes,[19] while **4**·MeTHF exhibits diagnostically reduced *g*-anisotropy (g_1 = 2.496, g_2 = 2.336, g_3 = 1.971; A_1 = 121 MHz, A_2 = 131 MHz, A_3 = 128 MHz from coupling to ^{103}Rh).[12]

Treatment of bulk microcrystalline **4** with H_2 (1 atm) at room temperature resulted in a rapid color change from dark purple to pastel pink, with concomitant liberation of methane verified by analysis of the head space by GC-TCD within 1 h (Figure 3). Conversion into the target rhodium(II) hydride **1** is supported by appearance of a metal-hydride band in the ATR IR spectrum at 1941 cm^{-1}, and repeating the reaction using an ensemble of single crystals of **4** enabled structural elucidation of the product by X-ray diffraction following a single-crystal to single-crystal transformation (1 atm H_2, RT for 2 h). Statistically significant contractions of the Rh1–P2 (2.2898(6) vs 2.3160(5) Å), Rh1–P3 (2.2910(6) vs 2.3148(5) Å), and Rh1–N20 bonds (2.134(2) vs 2.151(2) Å) are measured relative to **4**, and the hydride ligand in **1** was located from the Fourier difference map and refined with residual electron density at this coordination site <0.3 eÅ^3 (Figure S35). Decomposition into a diamagnetic mixture of **3** (δ 82.4, $^1J_{RhH}$ = 120 Hz) and $[Rh(PNP\text{-}t\text{Bu})(MeTHF)][BAr^F_4]$ **5** (δ 65.1, $^1J_{RhH}$ = 146 Hz; verified by independent synthesis) was observed upon dissolution of **1** in MeTHF at room temperature, with an initial rate and isotope labeling study consistent with bimetallic reductive elimination of H_2[10] and concurrent, but slower, H atom extraction from the solvent (>95% decomposition within 90 min, 10 mM initial concentration). Formation of **1** was nevertheless verified in frozen MeTHF glass solution by EPR spectroscopy at 115 K through preparation of the sample in thawing MeTHF, as gauged by significant perturbations to the **g**-tensor and the extent of hyperfine coupling (g_1 = 3.246, g_2 = 2.351, g_3 = 1.825; A_1 = 291 MHz, A_2 = 195 MHz, A_3 = 187 MHz from coupling to ^{103}Rh; Figure 3A). Installation of the hydride ligands is notably supported by spectroscopic resolution of ^{1}H coupling of 40 MHz along the g_3 component of the respective solvent

https://doi.org/10.1021/acs.inorgchem.6c04272
Inorg. Chem. XXXX, XXX, XXX−XXX

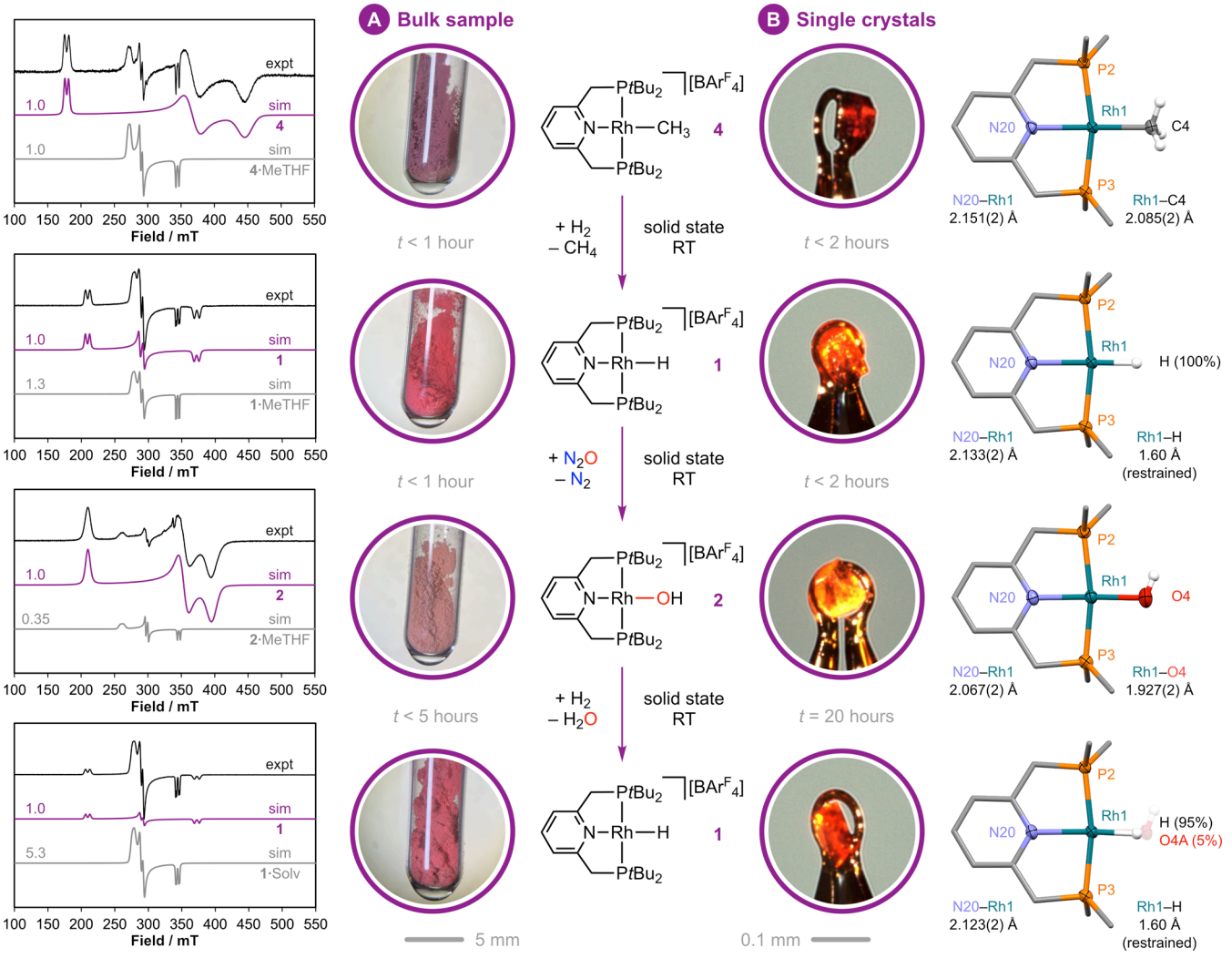

Figure 3. Gas/solid transformations of rhodium(II) complexes **1**, **2**, and **4** using (A) bulk microcrystalline and (B) single crystal samples, with supporting EPR and crystallographic data. CW X-band EPR spectra were recorded at 115 K using frozen MeTHF glass solutions prepared by dissolution of the sample in thawing MeTHF. Simulated spectra of square planar rhodium(II) complexes in purple and corresponding solvent adducts in gray (Solv = H_2O/MeTHF mixture). Truncated solid-state structures shown with selected thermal ellipsoids at 50% probability; counterion and most H atoms omitted for clarity. Additional metrics: **1**, Rh1–P2, 2.2898(6) Å; Rh1–P3, 2.2910(6) Å; P2–Rh1–P3, 168.07(2)°; N20–Rh1–H, 178.98(6)°; **2**, Rh1–P2, 2.3113(7) Å; Rh1–P3, 2.3069(7) Å; P2–Rh1–P3, 168.43(2)°; N20–Rh1–O4, 177.85(9)°; **2** + H_2 (20 h), Rh1–P2, 2.2920(6) Å; Rh1–P3, 2.2909(6) Å; P2–Rh1–P3, 168.16(2)°; N20–Rh1–H/O4A, 177.2(13)/179.0(11)°.

adduct **1**·MeTHF, which is formed with a **1**:**1**·MeTHF ratio of 1.0:1.3 in this case (g_1 = 2.446, g_2 = 2.336, g_3 = 1.975; A_1 = 133 MHz, A_2 = 139 MHz, A_3 = 126 MHz from coupling to ^{103}Rh).

The reaction between **1** and N_2O (1 atm) was thereafter assessed using the samples prepared from **4** as described above. Rapid formation of a light peach microcrystalline powder was observed alongside disappearance of the metal-hydride band in the ATR IR spectrum and generation of N_2 in the headspace within 1 h (Figure 3). Selective formation of a new square planar rhodium(II) species is evident from EPR analysis of the bulk microcrystalline sample in frozen MeTHF glass solution at 115 K, and assignment as rhodium(II) hydroxide **2** was verified *in crystallo* by single-crystal X-ray diffraction (1 atm N_2O, RT for 2 h). The solid-state structure is notable for a Rh1–O4 bond length of 1.927(3) Å and a reduction in the *trans* Rh1–N20 bond length (2.067(2) vs 2.133(2) Å). Complex **2** is significantly less stable than **1** in solution, decomposing in <5 min upon dissolution in MeTHF at room temperature, but only EPR signatures for **2** (g_1 = 3.231, g_2 = 1.921, g_3 = 1.716; coupling to ^{103}Rh not resolved) and **2**·MeTHF (g_1 = 2.601, g_2 = 2.276, g_3 = 1.961; A_1 = 182 MHz, A_2 = 126 MHz, A_3 = 119 MHz from coupling to ^{103}Rh) in a 1:0.35 ratio were observed when the sample was prepared in thawing MeTHF.

The stepwise hydrogenation of N_2O was subsequently realized by treatment of **2** with H_2 (1 atm) in the solid state at room temperature, although reformation of **1** and loss of H_2O was slower than the preceding two gas/solid reactions. For the bulk microcrystalline sample, analysis by EPR spectroscopy (115 K, frozen MeTHF glasses) indicated that between 1 to 5 h is required for complete conversion of **2** into **1**. Generation of 1 equiv of water was corroborated by ^{1}H NMR spectroscopy following quenching the metalloradical with CO and dissolving the reaction mixture in THF.[20] Rhodium(I) carbonyl complex [Rh(PNP-*t*Bu)(CO)][BAr^F_4] **6** was produced and, consistent with Rh–O bond hydrogenolysis by direct reaction with H_2, when the reaction of **2** was repeated with D_2, no H/D scrambling was observed in the methylene

https://doi.org/10.1021/acs.inorgchem.6c04272
Inorg. Chem. XXXX, XXX, XXX–XXX

bridges of pincer ligand backbone (nor other sites).[5] The rate of hydrogenolysis is appreciably slower when performed using single crystals of **2** (ca. 95% conversion after 20 h) and attributed to a reduction in surface area. Such effects are well-documented in solid-state molecular organometallic chemistry.[15] Retention of crystallinity and ejection of water from the lattice following three single-crystal to single-crystal transformations is nevertheless quite remarkable![21]

Having verified the stoichiometric hydrogenation of N_2O *in crystallo*, the catalytic hydrogenation of N_2O harnessing this gas/solid reactivity was assessed on a small scale using microcrystalline **4** as the precatalyst and a 1:1 mixture of N_2O and H_2 (2 atm) at room temperature for 48 h.[21] Liberation of CH_4 and reduction of N_2O to N_2 were observed in the headspace, and an apparent turnover number of 8.3 was quantified by GC-TCD using methane as the internal standard (averaged over duplicate runs). Following quenching with CO, the reaction mixture was analyzed by ^{31}P NMR spectroscopy for phosphine oxide to signpost the formation of rhodium nanoparticles.[7] However, consistent with the N_2O hydrogenation being catalyzed by the rhodium(II)-based molecular material, **6** was the only phosphorus-containing species observed.

In summary, solid-state organometallic methods have been used to access a highly reactive rhodium(II) hydride complex and assess its application in the hydrogenation of N_2O. Through successive gas/solid transformations a reaction sequence involving Rh(II)−CH_3 → Rh(II)−H → Rh(II)−OH → Rh(II)−H bond interconversions has been structurally mapped out by single-crystal X-ray diffraction, with the identity of the metalloradicals involved verified by EPR spectroscopy. Hydrogenolysis of the rhodium(II) hydroxide proceeds more slowly than reaction of the rhodium(II) hydride with nitrous oxide, and an isotope labeling study is consistent with direct reaction with H_2 rather than an alternative bifunctional mechanism. The rhodium metalloradicals are sufficiently robust to promote the catalytic hydrogenation of N_2O at room temperature, with an apparent turnover >8 and turnover limiting Rh−O bond hydrogenolysis inferred from relative rate of the stoichiometric transformations. While the reduction of N_2O using H_2 is not a practical remediation method,[6,22] this transformation is of fundamental importance for learning how to design efficient catalysts for the abatement and repurposing of N_2O. This work highlights the potential of site-isolated late transition-metal metalloradicals to engage in productive catalytic reactivity.

SAFETY STATEMENT

Caution! Mixtures of N_2O and H_2 are potentially explosive and should be handled with extreme care. This risk is compounded by the potential to form explosive mixtures of O_2 and H_2 in the presence of a metal catalyst. Hydrogenation reactions were performed on the smallest practical scale under relatively mild conditions behind a blast shield as described in the Supporting Information.

ASSOCIATED CONTENT

Supporting Information

The Supporting Information is available free of charge at https://pubs.acs.org/doi/10.1021/acs.inorgchem.6c04272.

Full experimental details and selected spectroscopic and crystallographic data[23] (PDF)

Accession Codes

Deposition Numbers 2564403−2564408 contain the supplementary crystallographic data for this paper. These data can be obtained free of charge via the joint Cambridge Crystallographic Data Centre (CCDC) and Fachinformationszentrum Karlsruhe Access Structures service.

AUTHOR INFORMATION

Corresponding Authors

Adrian B. Chaplin − *Department of Chemistry, University of Warwick, Coventry CV4 7AL, U.K.;* orcid.org/0000-0003-4286-8791; Email: a.b.chaplin@warwick.ac.uk

Emma Richards − *School of Chemistry, Cardiff University, Translational Research Hub, Cardiff CF24 4HQ, U.K.;* orcid.org/0000-0001-6691-2377; Email: richardse10@cardiff.ac.uk

Authors

Thomas M. Hood − *Department of Chemistry, University of Warwick, Coventry CV4 7AL, U.K.;* orcid.org/0000-0003-2506-2753

Sophie H. Dewick − *Department of Chemistry, University of Warwick, Coventry CV4 7AL, U.K.*

Jie Liu − *Department of Physics, University of Warwick, Coventry CV4 7AL, U.K.;* orcid.org/0000-0002-1301-057X

Complete contact information is available at: https://pubs.acs.org/10.1021/acs.inorgchem.6c04272

Notes

The authors declare no competing financial interest.

ACKNOWLEDGMENTS

This work was supported by NERC grants NE/S007350/1 (CENTA2 studentship to SHD) and NE/X018377/1. We also acknowledge funding from the Leverhulme Trust (RPG-2022-214, TMH), Cardiff University and the University of Warwick. Single-crystal and powder X-ray diffraction experiments were carried out using equipment provided by the University of Warwick X-ray Diffraction Research Technology Platform.

REFERENCES

(1) (a) Calvin, K.; Dasgupta, D.; Krinner, G.; Mukherji, A.; Thorne, P. W.; Trisos, C.; Romero, J.; Aldunce, P.; Barrett, K.; Blanco, G.; Cheung, W. W. L.; Connors, S.; Denton, F.; Diongue-Niang, A.; Dodman, D.; Garschagen, M.; Geden, O.; Hayward, B.; Jones, C.; Jotzo, F.; Krug, T.; Lasco, R.; Lee, Y.-Y.; Masson-Delmotte, V.; Meinshausen, M.; Mintenbeck, K.; Mokssit, A.; Otto, F. E. L.; Pathak, M.; Pirani, A.; Poloczanska, E.; Pörtner, H.-O.; Revi, A.; Roberts, D. C.; Roy, J.; Ruane, A. C.; Skea, J.; Shukla, P. R.; Slade, R.; Slangen, A.; Sokona, Y.; Sörensson, A. A.; Tignor, M.; Vuuren, D. van.; Wei, Y.-M.; Winkler, H.; Zhai, P.; Zommers, Z.; Hourcade, J.-C.; Johnson, F. X.; Pachauri, S.; Simpson, N. P.; Singh, C.; Thomas, A.; Totin, E.; Alegría, A.; Armour, K.; Bednar-Friedl, B.; Blok, K.; Cissé, G.; Dentener, F.; Eriksen, S.; Fischer, E.; Garner, G.; Guivarch, C.; Haasnoot, M.; Hansen, G.; Hauser, M.; Hawkins, E.; Hermans, T.; Kopp, R.; Leprince-Ringuet, N.; Lewis, J.; Ley, D.; Ludden, C.; Niamir, L.; Nicholls, Z.; Some, S.; Szopa, S.; Trewin, B.; Wijst, K.-I. v. d.; Winter, G.; Witting, M.; Birt, A.; Ha, M. *Climate Change 2023: Synthesis Report. Contribution of Working Groups I, II and III to the Sixth Assessment Report of the Intergovernmental Panel on Climate Change (IPCC)*; Core Writing Team, Lee, H., Romero, J., Eds.; IPCC: Geneva, Switzerland, 2023. (b) Ravishankara, A. R.; Daniel, J. S.;

Portmann, R. W. Nitrous Oxide (N_2O): The Dominant Ozone-Depleting Substance Emitted in the 21st Century. *Science* **2009**, *326*, 123−125.
(2) Pauleta, S. R.; Carepo, M. S. P.; Moura, I. Source and Reduction of Nitrous Oxide. *Coord. Chem. Rev.* **2019**, *387*, 436−449.
(3) (a) Cant, N. W.; Chambers, D. C.; Liu, I. O. Y. The Reduction of $^{15}N^{14}NO$ by CO and by H_2 over Rh/SiO_2: A Test of a Mechanistic Proposal. *J. Catal.* **2011**, *278*, 162−166. (b) Gluhoi, A. C.; Dekkers, M. A. P.; Nieuwenhuys, B. E. Comparative Studies of the N_2O/H_2, N_2O/CO, H_2/O_2 and CO/O_2 Reactions on Supported Gold Catalysts: Effect of the Addition of Various Oxides. *J. Catal.* **2003**, *219*, 197−205. (c) Carabineiro, S. A.; Nieuwenhuys, B. E. Reduction of N_2O by H_2 on the Ir(110) Surface: Oscillations in Rate. *Surf. Sci.* **2001**, *495*, 1−7. (d) Miyamoto, A.; Baba, S.; Mori, M.; Murakami, Y. Kinetics, Kinetic Deuterium Isotope Effects, and Mechanism of Nitrous Oxide Reaction with Hydrogen on Supported Precious-Metal Catalysts. *J. Phys. Chem.* **1981**, *85*, 3117−3122. (e) Roy, S.; Hegde, M. S.; Sharma, S.; Lalla, N. P.; Marimuthu, A.; Madras, G. Low Temperature NO_x and N_2O Reduction by H_2: Mechanism and Development of New Nano-Catalysts. *Appl. Catal. B: Environ.* **2008**, *84*, 341−350. (f) Vance, J. E.; Dixon, J. K. The Reaction between Nitrous Oxide and Hydrogen on Alumina. *J. Am. Chem. Soc.* **1941**, *63*, 176−181. (g) Dixon, J. K.; Vance, J. E. The Reaction between Nitrous Oxide and Hydrogen on Platinum. *J. Am. Chem. Soc.* **1935**, *57*, 818−821. (h) Cassel, H.; Glückauf, E. Über Den Verlauf Der Reaktion Zwischen Stickoxydul Und Wasserstoff Am Platinkontakt. *Z. für Phys. Chem.* **1932**, *19B*, 47−62. (i) Hinshelwood, C. N. The Kinetics of the Interaction of Nitrous Oxide and Hydrogen. *Proc. R. Soc. London, Ser. A* **1924**, *106*, 292−298.
(4) (a) Bermejo, J.; Ortega-Lepe, I.; Santos, L. L.; Rendón, N.; López-Serrano, J.; Álvarez, E.; Suárez, A. Nitrous Oxide Activation by Picoline-Derived Ni−CNP Hydrides. *Chem. Commun.* **2024**, *60*, 1575−1578. (b) Kohl, S. W.; Weiner, L.; Schwartsburd, L.; Konstantinovski, L.; Shimon, L. J. W.; Ben-David, Y.; Iron, M. A.; Milstein, D. Consecutive Thermal H_2 and Light-Induced O_2 Evolution from Water Promoted by a Metal Complex. *Science* **2009**, *324*, 74−77. (c) Lee, J.-H.; Pink, M.; Tomaszewski, J.; Fan, H.; Caulton, K. G. Facile Hydrogenation of N_2O by an Operationally Unsaturated Osmium Polyhydride. *J. Am. Chem. Soc.* **2007**, *129*, 8706−8707. (d) Kaplan, A. W.; Bergman, R. G. Nitrous Oxide Mediated Synthesis of Monomeric Hydroxoruthenium Complexes. Reactivity of $(DMPE)_2Ru(H)(OH)$ and the Synthesis of a Silica-Bound Ruthenium Complex. *Organometallics* **1998**, *17*, 5072−5085. (e) Kaplan, A. W.; Bergman, R. G. Nitrous Oxide Mediated Oxygen Atom Insertion into a Ruthenium−Hydride Bond. Synthesis and Reactivity of the Monomeric Hydroxoruthenium Complex $(DMPE)_2Ru(H)(OH)$. *Organometallics* **1997**, *16*, 1106−1108. (f) Vaughan, G. A.; Rupert, P. B.; Hillhouse, G. L. Selective O-Atom Transfer from Nitrous Oxide to Hydride and Aryl Ligands of Bis(Pentamethylcyclopentadienyl)Hafnium Derivatives. *J. Am. Chem. Soc.* **1987**, *109*, 5538−5539.
(5) Zeng, R.; Feller, M.; Ben-David, Y.; Milstein, D. Hydrogenation and Hydrosilylation of Nitrous Oxide Homogeneously Catalyzed by a Metal Complex. *J. Am. Chem. Soc.* **2017**, *139*, 5720−5723.
(6) Nappen, S. T.; Gamboa-Carballo, J. J.; Tschanen, E.; Ricatto, F.; Wörle, M. D.; Thomas, A.; Trincado, M.; Grützmacher, H. Water Serving as Cocatalyst for the Highly Efficient Homogeneously Catalyzed Conversion of N_2O/H_2 Mixtures with Optimized Rhodium NHC Complexes. *Angew. Chem., Int. Ed.* **2025**, *64*, No. e202502616.
(7) Dewick, S. H.; Hood, T. M.; Han, Y.; Huband, S.; Chaplin, A. B. Rhodium-Catalysed Hydrogenation of Nitrous Oxide. *Catal. Sci. Technol.* **2025**, *15*, 4126−4129.
(8) (a) Ortega-Lepe, I.; Sánchez, P.; Santos, L. L.; Lara, P.; Rendón, N.; López-Serrano, J.; Salazar-Pereda, V.; Álvarez, E.; Paneque, M.; Suárez, A. Catalytic Nitrous Oxide Reduction with H_2 Mediated by Pincer Ir Complexes. *Inorg. Chem.* **2022**, *61*, 18590−18600. (b) Jurt, P.; Abels, A. S.; Gamboa-Carballo, J. J.; Fernández, I.; Le Corre, G.; Aebli, M.; Baker, M. G.; Eiler, F.; Müller, F.; Wörle, M.; Verel, R.; Gauthier, S.; Trincado, M.; Gianetti, T. L.; Grützmacher, H. Reduction of Nitrogen Oxides by Hydrogen with Rhodium(I)−Platinum(II) Olefin Complexes as Catalysts. *Angew. Chem., Int. Ed.* **2021**, *60*, 25372−25380.
(9) (a) Ardon, Y.; Malakar, S.; Keller, T. M.; Gau, M. R.; Goldberg, K. I. Acid Catalyst Is Required for Hydrogenolysis of a Late Metal Hydroxo Complex. *J. Am. Chem. Soc.* **2025**, *147*, 46051−46060. (b) Bailey, W. D.; Phearman, A. S.; Luconi, L.; Rossin, A.; Yakhvarov, D. G.; D'Accolti, L.; Flowers, S. E.; Kaminsky, W.; Kemp, R. A.; Giambastiani, G.; Goldberg, K. I. Hydrogenolysis of Dinuclear PCN^R Ligated Pd^{II} μ-Hydroxides and Their Mononuclear Pd^{II} Hydroxide Analogues. *Chem.—Eur. J.* **2019**, *25*, 9920−9929. (c) Burgess, S. A.; Devarajan, D.; Bolaño, T.; Ess, D. H.; Gunnoe, T. B.; Sabat, M.; Myers, W. H. 1,2-Addition of Dihydrogen across Rhodium(III)−OMe Bonds. *Inorg. Chem.* **2014**, *53*, 5328−5340. (d) Fulmer, G. R.; Herndon, A. N.; Kaminsky, W.; Kemp, R. A.; Goldberg, K. I. Hydrogenolysis of Palladium(II) Hydroxide, Phenoxide, and Alkoxide Complexes. *J. Am. Chem. Soc.* **2011**, *133*, 17713−17726. (e) Gerber, R.; Fox, T.; Frech, C. M. P Csp^3 P and P Csp^2 P Palladium(II) Hydride Pincer Complexes: Small Structural Difference—Large Effect on Reactivity. *Chem.—Eur. J.* **2010**, *16*, 6771−6775. (f) Fulmer, G. R.; Muller, R. P.; Kemp, R. A.; Goldberg, K. I. Hydrogenolysis of Palladium(II) Hydroxide and Methoxide Pincer Complexes. *J. Am. Chem. Soc.* **2009**, *131*, 1346−1347. (g) Thompson, J. S.; Randall, S. L.; Atwood, J. D. Bond-Forming Reactions to an Iridium-Coordinated Hydroxo Group: Reaction of *trans*-$Ir(CO)(OH)[P(p\text{-tolyl})_3]_2$ with MeI, EtI, HCl, CH_3COCl, and H_2. *Organometallics* **1991**, *10*, 3906−3910. (h) Thompson, J. S.; Bernard, K. A.; Rappoli, B. J.; Atwood, J. D. Formation of Carbon-Hydrogen and Oxygen-Hydrogen Bonds at Iridium Centers: Addition of Hydrogen and Hydrogen Chloride to *trans*-$RIr(CO)L_2$(R = Me, OMe; L = PPh_3, $P(p\text{-tolyl})_3$). *Organometallics* **1990**, *9*, 2727−2731.
(10) Hidalgo, N.; Moreno, J. J.; García-Rubio, I.; Campos, J. Enhanced Dihydrogen Activation by Mononuclear Iridium(II) Compounds: A Mechanistic Study. *Angew. Chem., Int. Ed.* **2022**, *61*, No. e202206831.
(11) Pita-Milleiro, A.; Hidalgo, N.; Moreno, J. J.; Fernández, I.; Campos, J. An Open-Shell Ir(II)/Ir(IV) Redox Couple Outperforms an Ir(I)/Ir(III) Pair in Olefin Isomerization. *Nat. Chem.* **2025**, *17*, 606−613.
(12) Hood, T. M.; Dewick, S. H.; John, A.; Tidey, J. P.; Macpherson, J. V.; Bjornsson, R.; Richards, E.; Krämer, T.; Chaplin, A. B. Solvent-Dependent Carbon-to-Metal Hydrogen Atom Transfer Reactivity of a Square Planar Rhodium(II) Alkynyl Complex. *Organometallics* **2026**, *45*, 892−901.
(13) (a) Hood, T. M.; Ward, A. C. C.; Krämer, T.; Chaplin, A. B. Shedding Light on the Copper-Catalysed Diboron(4) Reduction of Nitrous Oxide. *Catal. Sci. Technol.* **2026**, *16*, 4744−4749. (b) Hood, T. M.; Charman, R. S. C.; Liptrot, D. J.; Chaplin, A. B. Copper(I) Catalysed Diboron(4) Reduction of Nitrous Oxide. *Angew. Chem., Int. Ed.* **2024**, *63*, No. e202411692. (c) Gyton, M. R.; Leforestier, B.; Chaplin, A. B. Rhodium(I) Pincer Complexes of Nitrous Oxide. *Angew. Chem., Int. Ed.* **2019**, *58*, 15295−15298.
(14) Menglet, D.; Bond, A. M.; Coutinho, K.; Dickson, R. S.; Lazarev, G. G.; Olsen, S. A.; Pilbrow, J. R. EPR, Electronic Spectra, and Electron Transfer Properties of the 17 Electron Carbonylhydrotris(Triphenylphosphine)Rhodium(II) Cation. *J. Am. Chem. Soc.* **1998**, *120*, 2086−2089.
(15) Altus, K. M.; Furfari, S. K.; Goodall, J. C.; Gyton, M. R.; Heaton, J. H.; Johnson, C. L.; McKay, A. I.; Møller, M. S.; Pike, S. D.; Weller, A. S. Solid-State Molecular Organometallic Chemistry (SMOM): A User Guide to in Crystallo Single-Crystal to Single-Crystal Transformations Using Solid/Gas Methods. *Dalton Trans.* **2026**, *55*, 6649−6666.
(16) (a) Reid, K. A.; Powers, D. C. Crystallo Organometallic Chemistry. *Chem. Commun.* **2021**, *57*, 4993−5003. (b) Pike, S. D.; Weller, A. S. Organometallic Synthesis, Reactivity and Catalysis in the Solid State Using Well-Defined Single-Site Species. *Philos. Trans. R. Soc. A* **2015**, *373*, 20140187.

(17) (a) Hanson, S. K.; Heinekey, D. M.; Goldberg, K. I. C−H Bond Activation by Rhodium(I) Phenoxide and Acetate Complexes: Mechanism of H−D Exchange between Arenes and Water. *Organometallics* **2008**, *27*, 1454−1463. (b) Kloek, S. M.; Heinekey, D. M.; Goldberg, K. I. C−H Bond Activation by Rhodium(I) Hydroxide and Phenoxide Complexes. *Angew. Chem., Int. Ed.* **2007**, *46*, 4736−4738.
(18) Evans, D. F. The Determination of the Paramagnetic Susceptibility of Substances in Solution by Nuclear Magnetic Resonance. *J. Chem. Soc.* **1959**, 2003−2005.
(19) (a) Böttcher, H.; Klüfers, P.; Mies, T.; Mayer, P. Synthesis and Molecular Structure of *trans*-$[RhCl_2(tBu_2PPh)_2]$: A Rare Example of a Mononuclear Rhodium(II) Complex. *Z. für Anorg. Allg. Chem.* **2018**, *644*, 1593−1597. (b) Scheibel, M. G.; Wu, Y.; Stuckl, A. C.; Krause, L.; Carl, E.; Stalke, D.; de Bruin, B.; Schneider, S. Synthesis and Reactivity of a Transient, Terminal Nitrido Complex of Rhodium. *J. Am. Chem. Soc.* **2013**, *135*, 17719−17722. (c) Gerisch, M.; Krumper, J. R.; Bergman, R. G.; Tilley, T. D. Rhodium(III) and Rhodium(II) Complexes of Novel Bis(Oxazoline) Pincer Ligands. *Organometallics* **2003**, *22*, 47−58. (d) Van Gaal, H.L.M.; Verlaak, J.M.J.; Posno, T. Oxidation of $RhCl\{P(C_6H_{11})_3\}_2$ and an E.P.R. Study of Some Rhodium(II) Complexes. *Inorg. Chim. Acta* **1977**, *23*, 43−51.
(20) Feller, M.; Ben-Ari, E.; Gupta, T.; Shimon, L. J. W.; Leitus, G.; Diskin-Posner, Y.; Weiner, L.; Milstein, D. Mononuclear Rh(II) PNP-Type Complexes. Structure and Reactivity. *Inorg. Chem.* **2007**, *46*, 10479−10490.
(21) For examples of consecutive/catalytic single-crystal to single-crystal transformations see: (a) Altus, K. M.; Shi, Y.; Probst, P.; Heaton, J. H.; Gyton, M. R.; Lari, L.; Buchmeiser, M. R.; Dyer, P. W.; Weller, A. S. Room Temperature Ethene to Propene (ETP) Tandem Catalysis Using Single Crystalline Solid-State Molecular Pre-Catalysts. *Angew. Chem., Int. Ed.* **2025**, *64*, No. e202419923. (b) Gyton, M. R.; Sajjad, M. A.; Storm, D. J.; Altus, K. M.; Goodall, J. C.; Johnson, C. L.; Page, S. J.; Edwards, A. J.; Piltz, R. O.; Duckett, S. B.; Macgregor, S. A.; Weller, A. S. An Operationally Unsaturated Iridium-Pincer Complex That C−H Activates Methane and Ethane in the Crystalline Solid-State. *J. Am. Chem. Soc.* **2025**, *147*, 8706−8719. (c) Johnson, C. L.; Storm, D. J.; Sajjad, M. A.; Gyton, M. R.; Duckett, S. B.; Macgregor, S. A.; Weller, A. S.; Navarro, M.; Campos, J. A Gold(I)−Acetylene Complex Synthesised Using Single-Crystal Reactivity. *Angew. Chem., Int. Ed.* **2024**, *63*, No. e202404264. (d) Lv, Z.-J.; Eisenlohr, K. A.; Naumann, R.; Reuter, T.; Verplancke, H.; Demeshko, S.; Herbst-Irmer, R.; Heinze, K.; Holthausen, M. C.; Schneider, S. Triplet Carbenes with Transition-Metal Substituents. *Nat. Chem.* **2024**, *16*, 1788−1793. (e) Patrick, E. A.; Bowden, M. E.; Erickson, J. D.; Bullock, R. M.; Tran, B. L. Single-Crystal to Single-Crystal Transformations: Stepwise CO_2 Insertions into Bridging Hydrides of $[(NHC)CuH]_2$ Complexes. *Angew. Chem., Int. Ed.* **2023**, *62*, No. e202304648. (f) Bukvic, A. J.; Burnage, A. L.; Tizzard, G. J.; Martínez-Martínez, A. J.; McKay, A. I.; Rees, N. H.; Tegner, B. E.; Krämer, T.; Fish, H.; Warren, M. R.; Coles, S. J.; Macgregor, S. A.; Weller, A. S. A Series of Crystallographically Characterized Linear and Branched σ-Alkane Complexes of Rhodium: From Propane to 3-Methylpentane. *J. Am. Chem. Soc.* **2021**, *143*, 5106−5120. (g) Chadwick, F. M.; McKay, A. I.; Martinez-Martinez, A. J.; Rees, N. H.; Krämer, T.; Macgregor, S. A.; Weller, A. S. Solid-State Molecular Organometallic Chemistry. Single-Crystal to Single-Crystal Reactivity and Catalysis with Light Hydrocarbon Substrates. *Chem. Sci.* **2017**, *8*, 6014−6029. (h) Zenkina, O. V.; Keske, E. C.; Wang, R.; Crudden, C. M. Double Single-Crystal-to-Single-Crystal Transformation and Small-Molecule Activation in Rhodium NHC Complexes. *Angew. Chem., Int. Ed.* **2011**, *50*, 8100−8104. (i) Huang, Z.; White, P. S.; Brookhart, M. Ligand Exchanges and Selective Catalytic Hydrogenation in Molecular Single Crystals. *Nature* **2010**, *465*, 598−601.
(22) (a) Wang, L.-Q.; Li, T.; Ma, H.-H. Explosion Behaviors of Hydrogen-Nitrous Oxide Mixtures at Reduced Initial Pressures. *Process Saf. Environ. Prot.* **2021**, *153*, 11−18. (b) Wang, L.-Q.; Ma, H.-H.; Shen, Z.-W. Explosion Characteristics of H_2/N_2O and CH_4/N_2O Diluted with N_2. *Fuel* **2020**, *260*, 116355.
(23) (a) Pike, S. D.; Crimmin, M. R.; Chaplin, A. B. Organometallic Chemistry Using Partially Fluorinated Benzenes. *Chem. Commun.* **2017**, *53*, 3615−3633. (b) Chávez, I.; Alvarez-Carena, A.; Molins, E.; Roig, A.; Maniukiewicz, W.; Arancibia, A.; Arancibia, V.; Brand, H.; Manuel Manríquez, J. Selective Oxidants for Organometallic Compounds Containing a Stabilising Anion of Highly Reactive Cations: $(3,5(CF_3)_2C_6H_3)_4B^-)Cp_2Fe^+$ and $(3,5(CF_3)_2C_6H_3)_4B^-)$-$Cp^*_2Fe^+$. *J. Organomet. Chem.* **2000**, *601*, 126−132. (c) Neumann, E.; Pfaltz, A. Synthesis and Characterization of Cationic Rhodium Complexes with Stable Silylenes. *Organometallics* **2005**, *24*, 2008−2011. (d) Pelczar, E. M.; Emge, T. J.; Krogh-Jespersen, K.; Goldman, A. S. Unusual Structural and Spectroscopic Features of Some PNP-Pincer Complexes of Iron. *Organometallics* **2008**, *27*, 5759−5767. (e) Gyton, M. R.; Hood, T. M.; Chaplin, A. B. A Convenient Method for the Generation of $\{Rh(PNP)\}^+$ and $\{Rh(PONOP)\}^+$ Fragments: Reversible Formation of Vinylidene Derivatives. *Dalton Trans.* **2019**, *48*, 2877−2880. (f) Pregosin, P. S. *NMR in Organometallic Chemistry*; Wiley, 2012; pp 251−254;. (g) Stoll, S.; Schweiger, A. EasySpin, a Comprehensive Software Package for Spectral Simulation and Analysis in EPR. *J. Magn. Reson.* **2006**, *178*, 42−55. (h) *CrysAlis PRO*; Rigaku Oxford Diffraction, 2026;. (i) Sheldrick, G. M. SHELXT − Integrated Space-Group and Crystal-Structure Determination. *Acta Crystallogr. A* **2015**, *71*, 3−8. (j) Sheldrick, G. M. Crystal Structure Refinement with SHELXL. *Acta Crystallogr.* **2015**, *C71*, 3−8. (k) Dolomanov, O. V.; Bourhis, L. J.; Gildea, R. J.; Howard, J. A. K.; Puschmann, H. OLEX2: A Complete Structure Solution, Refinement and Analysis Program. *J. Appl. Crystallogr.* **2009**, *42*, 339−341. (l) Lingafelter, E. C.; Zakrzewski, G. A.; Ghilardi, C. A. Structure of the Cobalt(III) and Cobalt(II) Complexes of the Cage Ligand 1,8-Bis(Fluoroboro)-2,7,9,14,15,20-Hexaoxa-3,6−10,13,16,19-Hexaaza-4,5,11,12,17,18-Hexamethylbicyclo[6.6.6]Eicosa-3,5,10,12,16,18-Hexaene. *J. Am. Chem. Soc.* **1971**, *93*, 4411−4415. (m) Hall, M. M.; Veeraraghavan, V. G.; Rubin, H.; Winchell, P. G. The Approximation of Symmetric X-ray Peaks by Pearson Type VII Distributions. *J. Appl. Crystallogr.* **1977**, *10*, 66−68. (n) Altomare, A.; Cuocci, C.; Giacovazzo, C.; Moliterni, A.; Rizzi, R.; Corriero, N.; Falcicchio, A. EXPO2013: A Kit of Tools for Phasing Crystal Structures from Powder Data. *J. Appl. Crystallogr.* **2013**, *46*, 1231−1235. (o) Chaplin, A. B.; Weller, A. S. $[Rh\{NC_5H_3\text{-}2,6\text{-}(CH_2P^tBu_2)_2\}(PCy_3)][BAr^F_4]$: A Latent Low-Coordinate Rhodium-(I) PNP Pincer Compound. *Organometallics* **2011**, *30*, 4466−4469.

https://doi.org/10.1021/acs.inorgchem.6c04272
Inorg. Chem. XXXX, XXX, XXX−XXX